Ionics (2014) 20:163–168
DOI 10.1007/s11581-013-0981-3

ORIGINAL PAPER

An improved carbonate precipitation method for the preparation of $Li_{1.2}Ni_{0.12}Co_{0.12}Mn_{0.56}O_2$ cathode material

Yanhong Xiang · Zhoulan Yin · Xinhai Li

Received: 7 April 2013 / Revised: 17 July 2013 / Accepted: 3 August 2013 / Published online: 21 August 2013

Abstract The precursor of $(Ni_{0.15}Co_{0.15}Mn_{0.7})CO_3$ has been synthesized by a carbonate precipitation method, which was used to prepare high-capacity cathode material $Li_{1.2}Ni_{0.12}Co_{0.12}Mn_{0.56}O_2$ for lithium-ion batteries. Carbonate precipitation was conducted using NH_4HCO_3 solution as the precipitation reagent. Two different feeding ways were adopted during the precipitation process. The physical properties of the precursor and the resulting $Li_{1.2}Ni_{0.12}Co_{0.12}Mn_{0.56}O_2$ were characterized in detail, and the electrochemical properties of the prepared $Li_{1.2}Ni_{0.12}Co_{0.12}Mn_{0.56}O_2$ powers were evaluated. It was found that the structural and morphological properties of the precursor and the final material were effectively improved by the ordered addition method. Electrochemical studies confirmed that the $Li_{1.2}Ni_{0.12}Co_{0.12}Mn_{0.56}O_2$ synthesized by ordered addition method exhibited a higher capacity of 287.3 mAh g^{-1}, and the capacity retention after 30 cycles was 90.5 %.

Keywords Lithium-ion battery · Cathode material · Lithium-rich material · Carbonate precipitation · Ordered addition method

Introduction

Layered lithium-rich transition metal oxides containing manganese, nickel, and cobalt are currently receiving worldwide attention as a possible replacement for the $LiCoO_2$ electrode of conventional lithium-ion cells [1–3]. These materials can be represented using either (1) structurally integrated two-component solid solution notations such as $xLi_2MnO_3 \cdot (1-x)LiMO_2$ (M=Ni, Co, and Mn) (layered layered in which the Li_2MnO_3 component is electrochemically activated above 4.4 V vs. Li/Li^+) or (2) standard notation as $Li_{1+y}M_{1-y}O_2$ (M=Ni, Co, and Mn) [4–7]. Several methods have been reported to prepare $Li_{1+y}M_{1-y}O_2$ (M=Ni, Co, and Mn) cathode materials, such as coprecipitation method [8–11], sol–gel method [12, 13], spray drying method [14], molten salt method [15], solid-state method [16], fast coprecipitation [17], etc. Among these methods, the coprecipitation method is the most commonly adopted to get phase pure oxide precursor with uniform and smaller particle size. However, as precipitation agent and complexing agent are mainly used to prepare the precursor with this method, the balance is difficult to control, and the precipitation efficiency is low. On the other hand, the performance of the materials is strongly correlated not only to the synthesis methods but also to the synthesis conditions. Therefore, it is necessary to explore an appropriate preparation method and optimize the process so that lithium-rich transition metal oxides with good performance can be prepared.

In this study, a carbonate precipitation method was attempted to prepare $Li_{1.2}Ni_{0.12}Co_{0.12}Mn_{0.56}O_2$ (which could be rewritten as $0.5Li_2MnO_3 \cdot 0.5LiNi_{0.3}Co_{0.3}Mn_{0.4}O_2$) cathode materials. The precursor, $(Ni_{0.15}Co_{0.15}Mn_{0.7})CO_3$, was prepared using NH_4HCO_3 solution as the precipitation reagent. Two different feeding ways were adopted during the precipitation process. The physical properties of the precursor and the resulting $Li_{1.2}Ni_{0.12}Co_{0.12}Mn_{0.56}O_2$ were characterized in detail, and the electrochemical properties of the prepared $Li_{1.2}Ni_{0.12}Co_{0.12}Mn_{0.56}O_2$ powers were evaluated.

Y. Xiang (✉) · Z. Yin
College of Chemistry and Chemical Engineering, Central South University, Changsha, Hunan 410083, People's Republic of China
e-mail: 112301009@csu.edu.cn

Z. Yin
e-mail: xhli@mail.csu.edu.cn

X. Li
School of Metallurgy and Environment, Central South University, Changsha, Hunan 410083, People's Republic of China

Experimental

Synthesis of $Li_{1.2}Ni_{0.12}Co_{0.12}Mn_{0.56}O_2$

$Li_{1.2}Ni_{0.12}Co_{0.12}Mn_{0.56}O_2$ was synthesized by calcination–crystallization process using carbonate precursor and lithium carbonate as raw materials. The carbonate precursor $(Ni_{0.15}Co_{0.15}Mn_{0.7})CO_3$ was synthesized in a continuously stirred tank reactor via a carbonate precipitation process. The precursor, $(Ni_{0.15}Co_{0.15}Mn_{0.7})CO_3$, was prepared according to the following methods: (a) stoichiometric amount of $NiSO_4{\cdot}6H_2O$, $CoSO_4{\cdot}7H_2O$, and $MnSO_4{\cdot}H_2O$ (Ni/Co/Mn= 0.15:0.15:0.7, molar ratio) was dissolved in distilled water with a concentration of 2.0 mol L^{-1}, respectively. The aqueous solution of $NiSO_4$, $MnSO_4$, and $CoSO_4$ was pumped into a continuously stirred tank reactor in sequence. At the same time, NH_4HCO_3 solution (2.0 mol L^{-1}) which was used as the precipitation reagent was continuously fed into the reactor. This method was named as ordered addition method. (b) Stoichiometric amount of $NiSO_4{\cdot}6H_2O$, $CoSO_4{\cdot}7H_2O$, and $MnSO_4{\cdot}H_2O$ (Ni/Co/Mn=0.15:0.15:0.7, molar ratio) was dissolved together in distilled water with a concentration of 2.0 mol L^{-1}. The mixed solution and a 2.0 mol L^{-1} NH_4HCO_3 solution were pumped into the reactor, respectively. This method was named as mixed addition method. Except for the feeding ways, the other experimental conditions were the same. The temperature of the reactor was maintained at 50 °C with continuous stirring for 12 h. The pH (7.5) value of the precipitation solution was maintained via carefully controlling the addition speed of the solutions. The precipitated powders were filtered and washed and then dried at 105 °C for 5 h. The obtained carbonate precursors were thoroughly mixed with a 3 at.% excess of a stoichiometric amount of Li_2CO_3 to compensate for the calcining loss and then calcined at 950 °C for 10 h in air. The precursors $(Ni_{0.15}Co_{0.15}Mn_{0.7})CO_3$ made from the ordered and mixed addition methods were marked as a' and b', respectively. The $Li_{1.2}Ni_{0.12}Co_{0.12}Mn_{0.56}O_2$ material made from the ordered and mixed addition methods were marked as a and b.

Measurements

X-ray diffraction measurements of materials were carried out on the Rigaku 2500 X-ray diffractometer using Cu-Kα radiation. The diffraction data were collected over the range $10° < 2\theta < 80°$. The chemical composition of the synthesized materials was determined by an atom absorption spectrophotometry (AAS) (TAS990; Beijing Purkinje General Instrument, China). The morphological characteristics of the samples were observed by a JEOL JSM-5600LV scanning electron microscopy (SEM). The active surface areas of the materials were measured by the Brunauer, Emmer, and Teller (BET) method with the Beishide Instrument, Beijing, China. Tap densities were determined using the ZA-201 tap density meter (Liaoning Instrument Research Institute Co., Ltd., Liaoning, China).

The cathode electrodes were prepared by mixing 80 wt% active material, 10 wt% carbon black as conductive material, and 10 wt% polyvinylidene difluoride binder in *N*-methyl-2-pyrrolidone solvent. Then, the slurry was cast onto an aluminum foil current collector, punched in the form of disks typically with a diameter of 14 mm and then dried. The charge–discharge tests were carried out using laboratory half-cell which consisted of a cathode and a lithium metal anode separated by the Celgard 2400 polyethylene/polypropylene film. Cells were assembled and sealed in an argon-filled glove box with the electrolyte of 1 mol L^{-1} $LiPF_6$ dissolved in EC/DMC/DEC (1:1:1 by volume). The charge–discharge tests were operated in the voltage range of 2.0–4.8 V with a constant current density of 15 mA g^{-1} (0.06 C) at room temperature on the LAND CT2001A battery test system (Jinnuo Wuhan Co., Ltd., People's Republic of China).

Results and discussion

Crystal structure properties

Figure 1 shows the X-ray diffraction (XRD) patterns of the $(Ni_{0.15}Co_{0.15}Mn_{0.7})CO_3$ precursors prepared by different feeding ways. All main characteristic peaks in each pattern were coincided with the diffraction peaks of hexagonal structure with a space group of $R\bar{3}c$ corresponding to $MnCO_3$ (JCPDS no. 44-1472), and no impurity-phase peaks exist. The peaks of sample a' were relatively broad which is likely due to the small grain size of the precursor particles [18], in agreement with the SEM image.

Figure 2 shows the XRD patterns of the $Li_{1.2}Ni_{0.12}Co_{0.12}Mn_{0.56}O_2$ samples synthesized by calcining the mixture

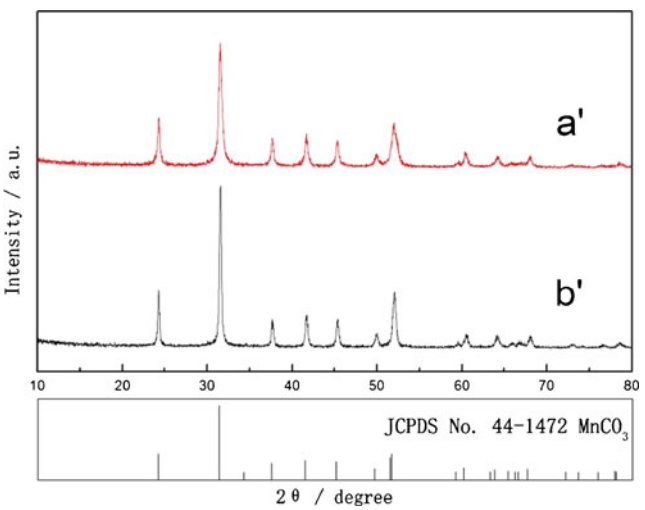

Fig. 1 XRD patterns of the $(Ni_{0.15}Co_{0.15}Mn_{0.7})CO_3$ precursors synthesized by different feeding ways: ordered addition method (*a'*) and mixed addition method (*b'*)

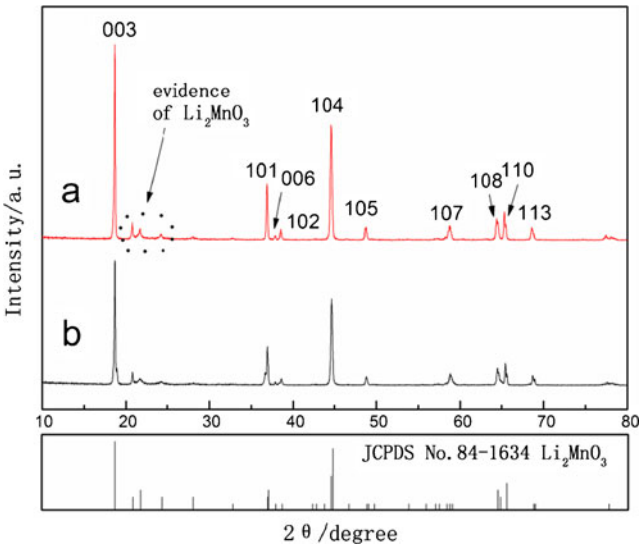

Fig. 2 XRD patterns of the $Li_{1.2}Ni_{0.12}Co_{0.12}Mn_{0.56}O_2$ samples synthesized from different precursors: *a* ordered addition method and *b* mixed addition method

of the precursors and lithium carbonate. Most of the XRD peaks in Fig. 2 were indexed with hexagonal α-$NaFeO_2$ structure (space group, $R\bar{3}m$) except for the weak peaks around 21° corresponding to integrated monoclinic Li_2MnO_3 phase ($C2/m$), originating from the ordering of Li^+ ion in the transition metal layer [3]. Another observation in the XRD patterns is the clear splitting of the (006)/(102) and (108)/(110) peaks, indicating that the material has a well-organized layered structure [19]. No peak of any impurity phase is detected in the XRD patterns, illustrating the high purity of the as-synthesized $Li_{1.2}Ni_{0.12}Co_{0.12}Mn_{0.56}O_2$ material prepared by these methods where the carbonate precipitation was conducted using NH_4HCO_3 solution as the precipitation reagent.

The ratio (R) of $I(003)/I(104)$ is sensitive to the cation distribution in lattice and the degree of cation mixing of materials [20–22]. When the R value is higher, the degree of cation mixing is lower. It was reported that the undesirable cation mixing would appear when R is smaller than 1.2. In our experiment, the R values of samples a and b are 1.701 and 1.432, respectively. The R value of $Li_{1.2}Ni_{0.12}Co_{0.12}Mn_{0.56}O_2$ sample prepared by ordered addition method is higher than that of the sample prepared by mixed addition method. In addition, the diffraction peaks in Fig. 2(a) are more sharp and narrow than those in Fig. 2(b). It reveals that the former has a better layered structure than the latter, which implies that the former might have better electrochemical performance. The possible reason for the structure difference could be attributed to the difference of the solubility product constants (K_{sp}) of $NiCO_3$, $CoCO_3$, and $MnCO_3$, i.e., $K_{sp}(NiCO_3)=6.6\times10^{-9}$, $K_{sp}(CoCO_3)=1.4\times10^{-13}$, and $K_{sp}(MnCO_3)=1.8\times10^{-11}$. Ni^{2+} is relatively difficult to precipitate completely compared to Mn^{2+} and Co^{2+} because of the relatively larger value of $K_{sp}(NiCO_3)$. In the ordered addition method, the precipitation reaction started with the formation of $NiCO_3$ seed particles and then dissolved reprecipitation according to the solubility equilibrium of precipitation between $NiCO_3$, $CoCO_3$, and $MnCO_3$ when $CoSO_4$ and $MnSO_4$ were pumped into the reactor in sequence and ended with the production of homogeneous particles of carbonate precursor with a chemical composition close to the nominal one. While in the mixed addition method, the carbonate precipitation reaction with Mn and Co dominated the whole reaction because of the relatively smaller value of $K_{sp}(MnCO_3)$ and $K_{sp}(CoCO_3)$, and then, the residual concentration of NH_3 was high in the solution, which would result in producing more nickel–ammonia complexes. This may result in nonuniform sedimentation with the mixed addition method. The assumption was confirmed by AAS results (Table 1) which shows that the measured molar ratios of Ni/Co/Mn are well in agreement to the intended composition for the sample a', while those for sample b' are slightly deviated from the target stoichiometry.

Morphology characteristics

The morphology of the precursors and the final $Li_{1.2}Ni_{0.12}Co_{0.12}Mn_{0.56}O_2$ samples is shown in Fig. 3. The particles of precursor a' (Fig. 3(a')) have uniform structural morphology and smooth crystal surface with narrow size distribution, which is in agreement with the XRD result (Fig. 1(a')), while the crystal size of sample b' (Fig. 3(b')) is bigger and is not as uniform. The possible explanation is that the transition metal ions were inconsistently precipitated easily due to the difference of the solubility product constant (K_{sp}) of $NiCO_3$, $CoCO_3$, and $MnCO_3$. After lithiation, the particles of sample b exist with some agglomeration. The morphology of sample a remains almost the same as that of the precursor powder except for some decrease in the diameter of the particle. This is consistent with the measurement results of the surface area by the BET method, 1.14 $m^2\ g^{-1}$ (sample a) and 0.81 $m^2\ g^{-1}$ (sample b), and the tap density of the samples a and b was 1.81 g cm^{-3} and 1.83 g cm^{-3}, respectively.

Electrochemical properties

Figure 4 shows the first charge–discharge profiles of the Li/$Li_{1.2}Ni_{0.12}Co_{0.12}Mn_{0.56}O_2$ samples. As can be seen, all charge

Table 1 Elementary analysis of the precursors prepared by different feeding ways: sample a', ordered addition method, and sample b', mixed addition method

	$n_{Ni}:n_{Co}:n_{Mn}$
Theoretical value	0.15:0.15:0.7
a'	(0.148±0.001):(0.149±0.001):(0.703±0.001)
b'	(0.146±0.001):(0.153±0.001):(0.701±0.001)

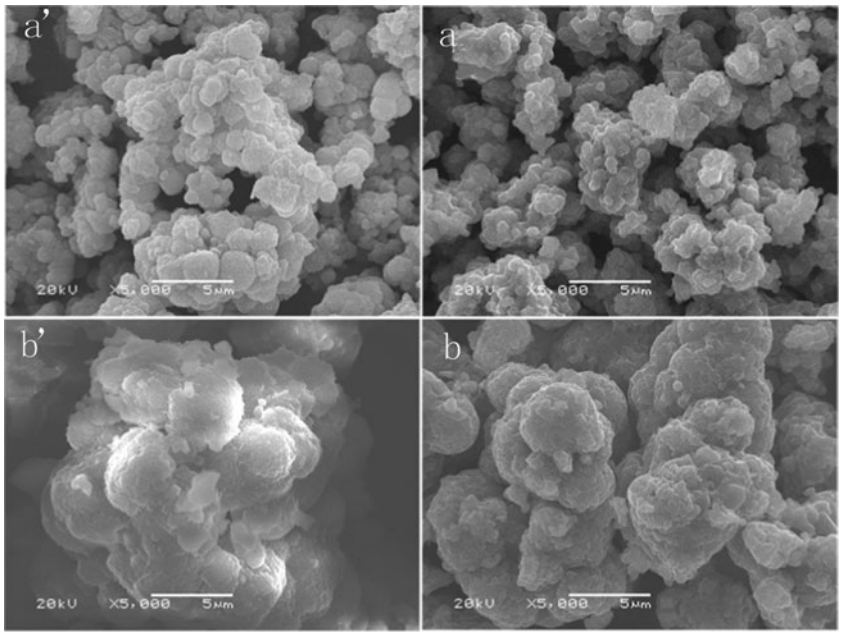

Fig. 3 The SEM images of the precursors prepared by different feeding ways and the $Li_{1.2}Ni_{0.12}Co_{0.12}Mn_{0.56}O_2$ samples calcined at 950 °C (ordered addition method (*a*, *a'*), mixed addition method (*b*, *b'*))

plots are composed of a slope region and a long plateau. The slope region (<4.5 V) is attributed to the extraction of Li^+ ions from the $LiNi_{0.3}Co_{0.3}Mn_{0.4}O_2$ component with a concomitant oxidation of Ni^{2+} and Co^{3+}. The long plateau, characterized by a voltage plateau above 4.5 V, is attributed to the removal of Li_2O from Li_2MnO_3 [10, 11]. Other workers also reported that the excess capacity originating at the 4.5 V plateau resulted from the hybridization of O^{2-} 2*p* orbital and Mn^{4+} 3*d* orbital [23]. The existence of the long plateau will ensure a high capacity in the subsequent cycling. All cells had first irreversible capacity. Some portion of the irreversible capacity may come from the oxidation of the electrolyte since the onset potential for the oxidation of electrolyte is at approximately 4.65 V, depending on the electrolyte composition. The large irreversible capacity loss may be related to the extraction of Li_2O followed by elimination of oxygen-ion vacancies from the lattice during first charge, resulting in a lower number of sites for insertion and extraction of Li^+ in the subsequent cycles [24]. Further, detailed structural and phase transitions associated with such lithiation–delithiation processes at higher voltage (>4.4 V) are not fully understood yet [6].

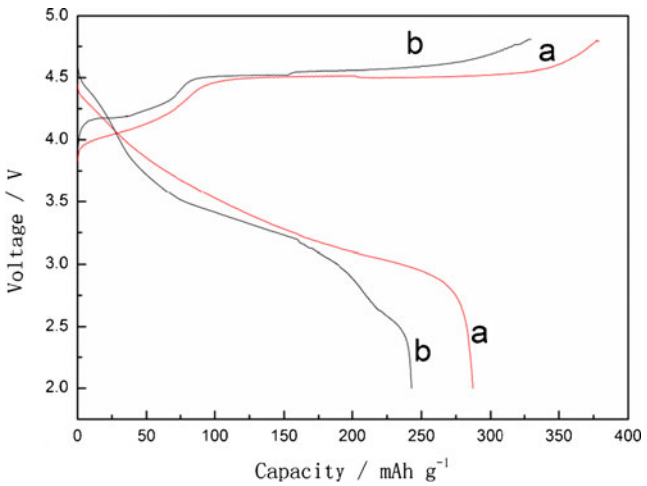

Fig. 4 Initial charge/discharge profiles for $Li/Li_{1.2}Ni_{0.12}Co_{0.12}Mn_{0.56}O_2$ cells at a specific current of 15 mA g^{-1} and at a voltage window of 2.0–4.8 V (*a* ordered addition method, *b* mixed addition method)

The sensitivity of the initial capacity to the synthesis conditions of the precursors is proved to be higher than the sensitivity of common powder XRD method, though the most substantial changes are indicated both by XRD and electrochemical capacity measurements. It can be seen from Fig. 4 that the discharge capacity of sample a (287.3 mAh g^{-1}) is greater than the common value (~250 mAh g^{-1}) of Li-rich transition metal oxide prepared by other methods [11, 25–28], while the value of sample b (242.8 mAh g^{-1}) is similar to the common value. Moreover, the coulombic efficiency of sample a is larger (75.76 %) than that of sample b (73.58 %).

Figure 5 shows the profiles of differential capacity (dQ/dV) versus voltage (V) for the $Li/Li_{1.2}Ni_{0.12}Co_{0.12}Mn_{0.56}O_2$ cells. The cells from both samples a and b have large oxidation peak (starting at 4.5 V) in differential capacity which corresponds to the 4.5 V plateau in Fig. 4. From Fig. 5(b), three cathodic peaks are evident on discharge curve. Although it is impossible to differentiate the reduction processes of the individual Mn, Ni, and Co ions from the data, it is believed that the reduction process at ~4.25 V may be associated with the occupation of tetrahedral sites by lithium within the extensively delithiated (lithium) layer and the lower voltage processes between 3.0 and 3.6 V to the occupation of octahedral sites [29]. Another cathodic peak below 2.75 V is consistent with the lithiation of a chemically derived MnO_2 component in the electrode. Such a voltage profile in $Li/Li_{1.2}Ni_{0.12}Co_{0.12}Mn_{0.56}O_2$ cell suggests that the layered structure

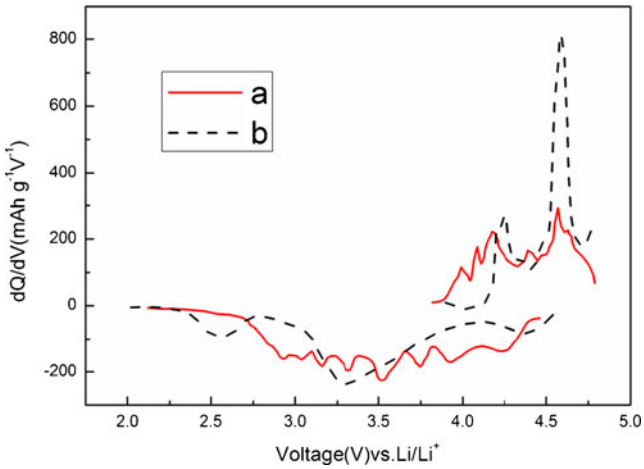

Fig. 5 Differential capacity versus voltage for Li/$Li_{1.2}Ni_{0.12}Co_{0.12}Mn_{0.56}O_2$ cells in the voltage range of 2.0–4.8 V (*a* ordered addition method, *b* mixed addition method)

transforms into a spinel phase during the charge process. This may attributed to the nonuniform sedimentation with the mixed addition method. Meanwhile, for the sample a, the cathodic peak of the cell below 2.75 V does not emerge. All the results indicate that the ordered addition method can guarantee the impurity of $Li_{1.2}Ni_{0.12}Co_{0.12}Mn_{0.56}O_2$ because of the difference of the solubility product constant (K_{sp}) of $NiCO_3$, $CoCO_3$, and $MnCO_3$.

The rate performance for the Li/$Li_{1.2}Ni_{0.12}Co_{0.12}Mn_{0.56}O_2$ cells is shown in Fig. 6. As can be seen, the discharge capacities of the sample a were higher than those of sample b at all different C rates. Moreover, the difference in capacity between samples a and b becomes greater as the discharge current rate is increased from 0.06 to 1 C. The good rate performance is attributed to the smaller particle size which shortens the migration path of lithium [17, 25]. However, further efforts are needed to improve the rate properties.

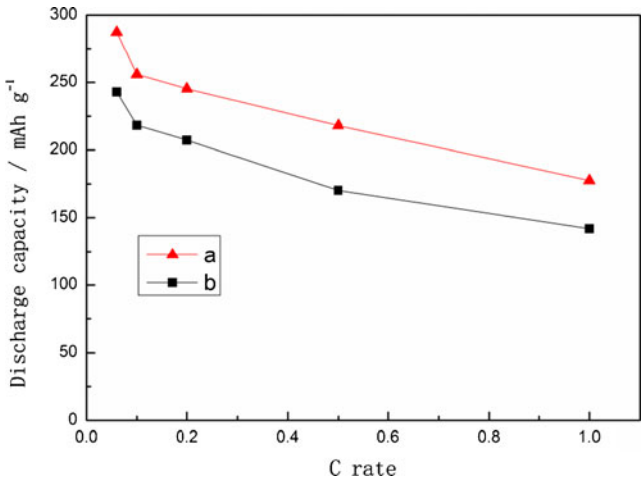

Fig. 6 The discharge capacities of Li/$Li_{1.2}Ni_{0.12}Co_{0.12}Mn_{0.56}O_2$ cells at different rates in the voltage range of 2–4.8 V (*a* ordered addition method, *b* mixed addition method)

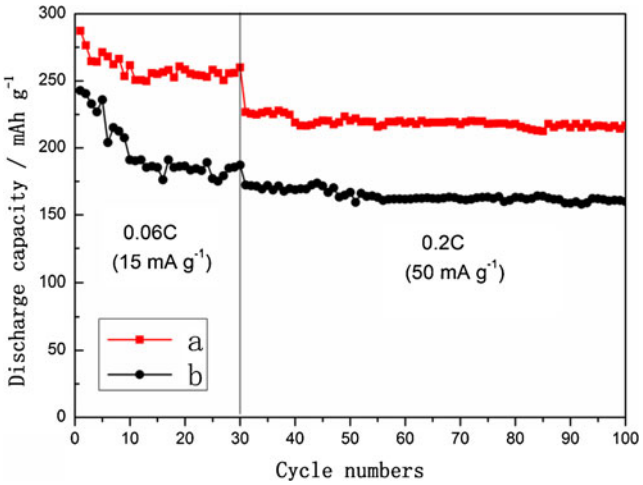

Fig. 7 Cycle performances of Li/$Li_{1.2}Ni_{0.12}Co_{0.12}Mn_{0.56}O_2$ cells in the voltage range of 2–4.8 V (*a* ordered addition method, *b* mixed addition method)

Figure 7 presents the cycling performance of the Li/$Li_{1.2}Ni_{0.12}Co_{0.12}Mn_{0.56}O_2$ cells. The cells were charged/discharged at a 0.06 C rate over the first 30 cycles and at a 0.2 C rate over the following 70 cycles. As can be seen, when cycled at 0.06 C, the discharge of sample a goes up and down at a steady high capacity (260 mAh g^{-1}), whereas the discharge of sample b has an unsteady lower capacity (190 mAh g^{-1}). The sample a delivers a capacity retention of 78.9 % after 100 cycles (30 cycles for 0.06 C and 70 cycles for 0.2 C), which is substantially higher than that of the sample b (65.9 %). The improved electrochemical characteristics may be attributed to the enhanced structural stability reflected by the higher *R* value, and the better layered structure of sample a is shown in Fig. 2(a). As reported by Thackeray [30], high crystallinity is essential to obtain good electrochemical properties and to maintain its structural integrity during cycling. The slight fluctuation in the capacity versus the cycle number plot is attributed to variations in the room temperature of the laboratory in which the tests were conducted.

The differences in the electrochemical performance of the $Li_{1.2}Ni_{0.12}Co_{0.12}Mn_{0.56}O_2$ cathode can be attributed to the differences in their physical and chemical properties such as the crystal structure and morphology. In this study, by using the ordered addition method with NH_4HCO_3 solution as the precipitation reagent, the physical and chemistry properties of the precursors and the $Li_{1.2}Ni_{0.12}Co_{0.12}Mn_{0.56}O_2$ cathode material were effectively improved, which results in the superior physical and electrochemical properties for $Li_{1.2}Ni_{0.12}Co_{0.12}Mn_{0.56}O_2$.

Conclusions

An improved carbonate precipitation method was employed to prepare the lithium-rich $Li_{1.2}Ni_{0.12}Co_{0.12}Mn_{0.56}O_2$ cathode

material. Carbonate precipitation was conducted using ordered addition method with NH_4HCO_3 solution as the precipitation reagent. The morphological and structural properties of the precursor and the final $Li_{1.2}Ni_{0.12}Co_{0.12}Mn_{0.56}O_2$ cathode material were effectively improved by the ordered addition method. Electrochemical studies confirmed that the $Li_{1.2}Ni_{0.12}Co_{0.12}Mn_{0.56}O_2$ synthesized by ordered addition method exhibited a higher capacity of 287.3 mAh g^{-1}, and the capacity retention after 30 cycles was 90.5 %. The results in this work suggest a simple and effective way to synthesize the lithium-rich cathode for rechargeable lithium batteries.

Acknowledgments This work was supported by the Hunan Provincial Innovation Foundation for Postgraduate, China, and the Major Science and Technology Project of Hunan Province, China (2011FJ1005).

References

1. Ellis BL, Lee KT, Nazar LF (2010) Chem Mater 22:691
2. Fergus JW (2010) J Power Sources 195:939
3. Thackeray MM, Kang SH, Johnson CS, Vaughey JT, Hackney SA (2006) Electrochem Commun 8:1531
4. Whittingham MS (2004) Chem Rev 104:4271
5. Croy JR, Kang SH, Balasubramanian M, Thackeray MM (2011) Electrochem Commun 13:1063
6. Marth SK, Nand J, Veith GM, Dudney NJ (2012) J Power Sources 199:220
7. Du K, Hu GR (2012) Chin Sci Bull (Chin Ver) 57:794
8. Zheng JM, Wu XB, Yang Y (2011) Electrochim Acta 56:3071
9. Lee DK, Park SH, Amine K, Bang HJ, Parakash J, Sun YK (2006) J Power Sources 162:1346
10. Park SH, Kang SH, Belharouak I, Sun YK, Amine K (2008) J Power Sources 77:177
11. Lim JH, Bang H, Lee KS, Amine K, Sun YK (2009) J Power Sources 189:571
12. Shin SS, Sun YK, Amine K (2002) J Power Sources 112:634
13. Kim JH, Sun YK (2003) J Power Sources 119–121:166
14. Zhang L, Muta T, Noguchi H, Wang X, Zhou M, Yoshio M (2003) J Power Sources 117:137
15. Zhao X, Cui Y, Xiao L, Liang H, Liu H (2011) Solid State Ionics 192:321
16. Yu L, Qiu W, Lian F, Liu W, Kang X, Huang J (2008) Mater Lett 62:3010
17. Chen Y, Xu G, Li J, Zhang Y, Chen Z, Kang F (2013) Electrochim Acta 87:686
18. Wang D, Belharouak I, Koenig GM Jr, Zhou G, Amine K (2011) J Mater Chem 21:9290
19. Wu F, Wang M, Su Y, Bao L, Chen S (2010) J Power Sources 195:2362
20. Manikandan P, Ananth MV, Kumar TP, Raju M, Periasamy P, Manimaran K (2011) J Power Sources 196:10148
21. Luo X, Wang X, Liao L, Wang X, Gamboa S, Sebastian PJ (2006) J Power Sources 161:601
22. Zhang B, Chen G, Xu P, Lv ZS (2007) Solid State Ionics 178:1230
23. Hong YS, Park YJ, Ryu KS, Chang SH (2005) Solid State Ionics 176:1035
24. Armstrong AR, Holzapfel M, Novák P, Johnson CS, Kang SH, Thackeray MM, Bruce PG (2006) J Am Chem Soc 128:8694
25. Wang J, Yuan G, Zhang M, Qiu B, Xia Y, Liu Z (2012) Electrochim Acta 66:61
26. Guo XJ, Li YX, Zheng M, Zheng JM, Li J, Gong ZL, Yang Y (2008) J Power Sources 184:414
27. Shojan J, Rao CV, Torres L, Singh G, Katiyar RS (2013) Mater Lett 104:57
28. Zhang J, Guo X, Yao S, Zhou W, Qiu X (2013) J Power Sources 238:245
29. Johnson CS, Li N, Lefief C, Vaughey JT, Thackeray MM (2008) Chem Mater 20:6095
30. Thackeray MM (1995) J Electrochem Soc 142:2558